JOURNAL OF GEOPHYSICAL RESEARCH, VOL. 101, NO. A3, PAGES 4825–4834, MARCH 1, 1996

Effect of coronal mass ejections on the structure of the heliospheric current sheet

Xuepu Zhao and J. Todd Hoeksema

W. W. Hansen Experimental Physics Laboratory, Center for Space Science and Astrophysics
Stanford University, Stanford, California

Abstract. The existence of a relatively stable large-scale heliospheric current sheet (HCS) structure near sunspot maximum has recently been questioned [*Hundhausen,* 1992]. We consider this question here by determining the effect of coronal mass ejections (CMEs) on the spiral characteristics of the interplanetary magnetic field (IMF) and on the HCS. In general, CMEs do not have long-term effects on the location of the HCS. The evidence shows that (1) the coronal streamer belt locally disrupted or blown out by CMEs reforms in a time interval shorter than the lifetime of the HCS structure; (2) the internal structure of IMF sector boundaries is temporarily changed during the passage of the interplanetary counterpart of CMEs; (3) even in the Carrington rotation just 1 month after the sunspot maximum of solar cycle 21 the IMF spiral characteristics are maintained, and the calculated sector pattern agrees very well with that observed at 1 AU; and (4) the fact that the calculated closed field regions correspond to the helmet streamers observed in the February 16, 1980, solar eclipse confirms the validity of the three-dimensional model even at high activity, giving additional confidence in the predicted HCS location. The rapid reformation of disrupted helmet structures may explain the existence of a structured HCS during intervals when CMEs occur frequently and several coronal helmet streamers along the base of the HCS are disrupted or blown out. Ulysses observations at the next sunspot maximum may finally answer the question.

1. Introduction

Understanding developed over nearly three 11-year sunspot cycles since the earliest spacecraft investigations indicates that near the ecliptic the interplanetary magnetic field (IMF) lies predominantly along an Archimedian spiral direction, that the spiral fields are organized into alternate sectors with field pointing toward and away from the Sun, and that the field direction reverses at relatively sharp sector boundaries in periods of a few minutes to a few hours [*Ness and Wilcox,* 1964; *Wilcox and Ness,* 1965; *Suess,* 1993] throughout most, if not all, of the solar cycle. The IMF sector structure results from the large-scale coronal field pattern in which positive polarity fields are separated from negative polarity fields by a warped, global current sheet, the heliospheric current sheet (HCS) [Schultz, 1973; *Smith et al.,* 1978]. The neutral line, i.e., the location of the coronal base of the HCS, can be approximately calculated by using the observed photospheric magnetic field together with the potential field–source surface model (PFSS) [e.g., *Wilcox et al.,* 1980; *Hoeksema et al.,* 1982, 1983; *Wang and Sheeley,* 1992; *Hoeksema and Zhao,* 1996]. It can also be mapped out with the maximum brightness curve of white light coronagraph synoptic charts in the declining, minimum, and ascending phases of the solar activity cycle [*Burlaga et al.,* 1981]. The HCS structure calculated from the PFSS model agrees with that mapped out from the white light synoptic chart [*Wilcox and Hundhausen,* 1983]. When the derived coronal magnetic field is coupled with an electron density model, the agreement becomes better [*Wang and Sheeley,* 1992]. The observed solar cycle variations in the in-ecliptic IMF sector structure manifest the changes in the inclination, shape, and topology of the calculated HCS. The sector pattern remains relatively stable in the late declining, minimum, and early rising phases of the sunspot cycle but shows less stability around maximum with changes in the number of sectors and in their sizes [*Hoeksema,* 1991].

The HCS forms where solar wind flows carrying magnetic fields of opposite polarity converge over magnetically closed regions of the corona, i.e., coronal helmet streamers. Since these same helmet streamers are the sites of some coronal mass ejections (CMEs) [*Hundhausen,* 1993], the following questions are raised: How do CMEs affect the HCS? Does the impossibility of mapping out the neutral line with the maximum brightness curve of white light coronagraph synoptic charts

Paper number 95JA03568.
0148-0227/96/95JA-03568$05.00

suggest the absence of the HCS at times of high activity when CMEs occur frequently [*Hundhausen,* 1992]? Recognizing that coronal helmet streamers are a source of CMEs, *Crooker et al.* [1993] suggest that the HCS is a conduit for outflow from (1) steady state helmet streamers, (2) small-scale ejections, and (3) large-scale CMEs. In other words, instead of a thin, disklike structure the thickness of the IMF polarity transition layer varies depending upon the number and activity of the helmet structures at its base.

CMEs cause observable changes in coronal structure, exhibiting various morphological features. CMEs can deflect, disrupt, or blow out preexisting coronal structures. Both SOLWIND and SMM observations showed that the most severe effect of CMEs on helmet streamers is a disruption or blowout of the preexisting density structure. A feature is considered to be disrupted if it survives the event but exhibits a "significant" change in shape, brightness, and/or location. A blowout is defined as the apparent disappearance of a structure after an event [*Howard et al,* 1985; *Burkepile and St Cyr,* 1993]. In the next section we determine the effect of disruption and blowout CMEs on the coronal streamer belt, using data near sunspot minimum.

Around the sunspot maximum of solar cycle 21 (December 1979) the ISEE 3 spacecraft was located at Earth's L1 point and provided continuous observations of the IMF and plasma properties. These high-quality data can be used to measure the effects of the interplanetary counterpart of CMEs (ICMEs) on sector boundaries and to identify the signature of the spiral magnetic field for each solar rotation. In addition, the solar eclipse observed on February 16, 1980, just after the sunspot maximum of solar cycle 21, provided a perspective view of the coronal magnetic field configuration. In sections 3 and 4 we will search for the effect of ICMEs on IMF sector boundaries and evidence for the existence of the HCS near sunspot maximum. We summarize and discuss the results in section 5.

2. Effect of CME on the Coronal Streamer Belt

As self-contained structures of plasma and magnetic fields, CMEs may be associated with changes in coronal structure on a large scale. The temporary and local effect of an individual CME on the coronal streamer belt has been described as a "bugle" on SMM white light synoptic charts where the band representing a coronal intensity structure brightens dramatically in the time interval leading up to an ejection and is exceptionally dim or almost nonexistent afterward (see Figure 10 of *Hundhausen* [1993]). In this paper we seek to determine whether these effects are generally permanent, lasting more than a solar rotation, or temporary. If the changes caused by most CMEs are permanent, the semistatic HCS location calculated from photospheric field will have no physical meaning during active periods.

The neutral line is usually calculated by using the potential field–source surface (PFSS) model. It has essentially the same structure as the coronal streamer belt obtained from the observed coronal polarization brightness [*Wilcox and Hundhausen,* 1983]. The neutral line calculated from the PFSS model and from the recently developed current sheet–source surface model [*Zhao and Hoeksema,* 1995] agrees with in situ in-ecliptic observations of the IMF polarity equally well [*Hoeksema and Zhao,* 1996]. So the effect of individual disruption and blowout CMEs should be visible in the HCS location calculated at the 2.5 R_s source surface by using the Wilcox Solar Observatory (WSO) photospheric field observations and the PFSS model with the radial field inner boundary condition [*Wang and Sheeley,* 1992; *Zhao and Hoeksema,* 1993]. Figure 1 displays the calculated neutral lines for Carrington rotations (CR) 1758 to 1767 in 1985, an interval just before solar minimum when the OMNItape has fewer IMF data gaps and SMM has more complete observations of CMEs. Superposed on Figure 1 are the positions of observed blowout CMEs (large open circles) and disruption CMEs (small open circles) as well as the calculated photospheric foot points (solid circles) of the open field lines on the source surface. Symbols plus and minus in Figure 1 denote daily magnetic polarity away from or toward the Sun. The polarities were observed at 1 AU and mapped back to the source surface, assuming a constant solar wind velocity resulting in a transit time of 5 days from the Sun to the Earth. The foot point areas approximate the locations of coronal holes [*Wang and Sheeley,* 1992], which are longer-lived than helmet streamers. As expected, the open circles cluster near the calculated neutral lines, and the predicted IMF polarity pattern agrees fairly well with the observed sector pattern. This fact confirms that the calculated neutral line is a fairly good representation of the coronal streamer belt near solar minimum. Figure 1 also shows that CMEs produced no significant long-term effect on the location of the coronal streamer belt, even though the temporary effect on individual helmet streamers was significant. This finding implies that the photospheric magnetic field is insensitive to CMEs and the disrupted or blown-out helmet structures reform in a time interval shorter than 27 days.

Other observations indicate that the reformation time of a blown-out helmet streamer is often much shorter than 27 days. For example, the coronal streamer belt seen in white light observations made at the west limb after a CME is basically the same as that seen at the east limb before the CME (see Figure 10 of *Hundhausen* [1993], suggesting a reformation time of less than 14 days. Yohkoh SXT observations indicate that magnetically closed helmet structures reform in a time interval as short as a couple of days [*Hiei et al.,* 1993].

The coronal streamer belt or the HCS is the boundary between adjacent coronal holes with opposite field polarity (see Figure 1); as such it shares the lifetime of ad-

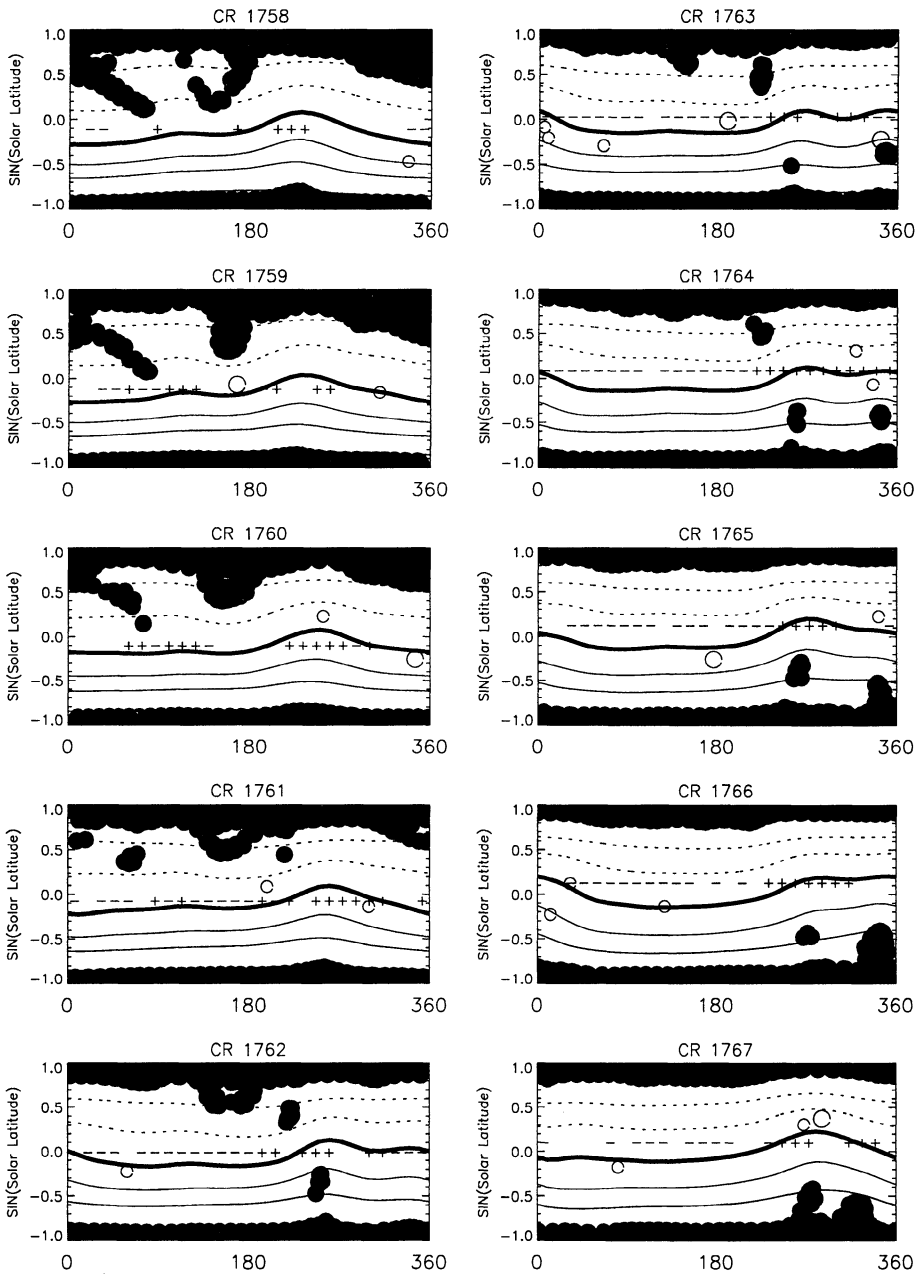

Figure 1. Comparison of the shape of the neutral lines (thick lines) before and after blowout CMEs (large open circles) and disruption CMEs (small open circles). The plus and minus symbols denote daily averaged outward and inward IMF polarity. The solid circles denote the foot points of open field lines (coronal holes).

jacent coronal holes. Coronal holes typically last several solar rotations throughout most of the solar cycle, much longer than the reformation time of disrupted or blown-out helmet streamers. Thus CMEs only temporarily and locally change the internal structure of the coronal streamer belt. That is why the coronal streamer belt and its quasi-stable structure can be approximately calculated by using the photospheric magnetic field, which is not expected to be significantly affected by CMEs.

3. Effect of ICMEs on IMF Sector Boundaries

The helical field lines in the ICMEs may be assumed to remain unentangled with the IMF spiral field lines, owing to polarization currents induced on the ICMEs' periphery. However, the induced polarization currents and the internal currents of a passing ICME may exert a large force on the ambient heliospheric currents near it.

Significant deformation (expansion) of the heliospheric current layer should be expected.

Counterstreaming halo electron events are believed to be the manifestation of the helical ICME fields and are among the most reliable indicators of CMEs in interplanetary space [*Gosling,* 1990]. By examing the variations of the IMF azimuthal angle during the passage of ICMEs we determine their effects on the HCS. The panels in the right column of Figure 2 display this angle for the first half of 1979 (CR 1678–1681), when ICMEs occurred infrequently enough that well-defined sector boundaries could still be observed. The hours when counterstreaming halo electron events were observed are indicated by solid rectangles at the 225° azimuth position. The panels on the left show the calculated neutral lines extrapolated to 1 AU and the observed daily IMF polarities (24-hour averages of the observed hourly azimuthal angles displayed on the right). To compare with in situ observations, the calculated neutral lines have been displaced 66° to account for the 5-day transit time of the neutral line from the source surface to the Earth. The good agreement between the predicted and observed IMF polarity patterns demonstrates the validity of the calculated location of the HCS less than 1 year before the sunspot maximum.

The well-defined sector boundary present near hour 90 of CR 1678 was expanded in the following rotation by an ICME with an associated shock (see the right column). It was significantly disturbed again by three events close to hour 90 in CR 1680 and finally reformed in CR 1681 when all the observed events had passed far beyond 1 AU. The events occurring near hour 380 of CR 1678 and 1679 have a similar effect on the sector boundary. The event near hour 510 of CR 1680 was located far from the calculated neutral line (see the left panel) and produced a change in azimuthal angle of less than 90°.

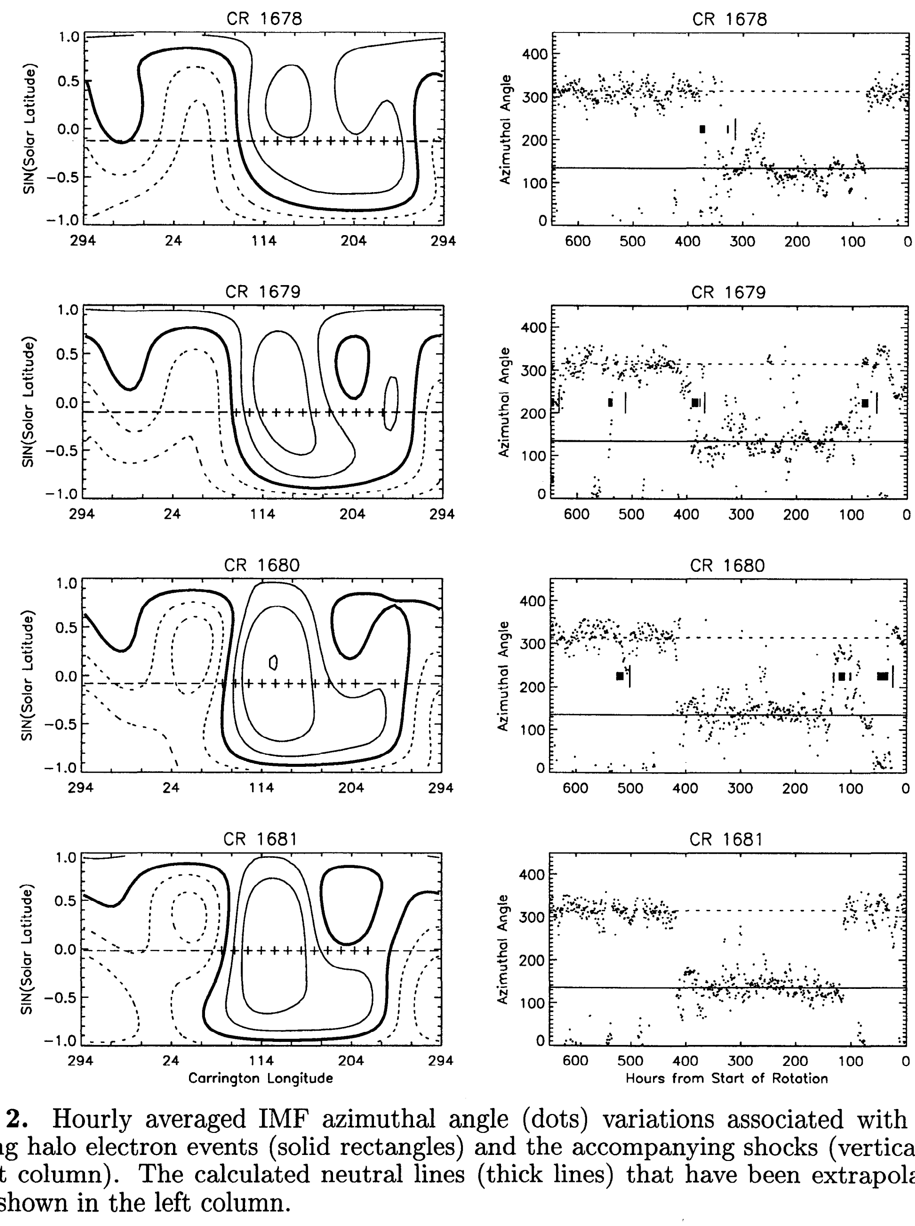

Figure 2. Hourly averaged IMF azimuthal angle (dots) variations associated with counterstreaming halo electron events (solid rectangles) and the accompanying shocks (vertical lines in the right column). The calculated neutral lines (thick lines) that have been extrapolated to 1 AU are shown in the left column.

Various attempts have been made to visualize the magnetic field topology of the coherent internal field rotations measured as magnetic clouds and certain other ICMEs pass over a spacecraft. The magnetic cloud observations have been consistently interpreted in terms of cylindrical magnetic flux ropes (twisted flux tubes) characterized by axial fields near their centers and increasingly poloidal fields near their outer edges [*Gosling,* 1990]. Most of the azimuthal angle changes associated with ICME passages presented in the right column of Figure 2 can be explained if we assume that the axes of embedded magnetic flux ropes are locally parallel to the appropriate segment of the neutral lines shown in the left column, and that the ropes propagate away from the Sun radially when the appropriate segment of the neutral line is parallel to the Sun's equator and azimuthally as well as radially when the segment is perpendicular to the equator owing to the corotation of the perpendicular HCS with the Sun. For instance, if the magnetic rope corresponding to the ICME near hour 400 of CR 1679 is centered on and parallel to the calculated neutral line near 84° Carrington longitude, the magnetic field near the outer edges of the rope must point outward on the right side of the axis and inward on the left side, on the basis of the ambient IMF polarity adjacent to the neutral line (see Figure 3a). In this case the rope propagates away from the Sun both radially and azimuthally, and the spacecraft would first observe an azimuth of ~135° at right-front of the rope as shown in Figure 3a. The observed azimuth would increase inside the rope and finally reach ~ 315° at left-rear of the rope where the spacecraft exits the rope. This is just what the ISEE spacecraft observed near hour 400 of CR 1679. The same picture works for the event near hour 90 of CR 1679 with the rope field configuration shown in Figure 3b. The change of the azimuthal angle less than 90° (between 315° and 225°) observed near hour 510 of CR 1680 can also be understood if the corresponding rope axis is parallel to the calculated neutral line near 24° Carrington longitude (see Figure 3c). In this case the segment of the neutral line is locally parallel to the Sun's equator, and ISEE 3 passed nearly radially from front to rear through only the lower part of the rope, where the field is pointed entirely toward the Sun.

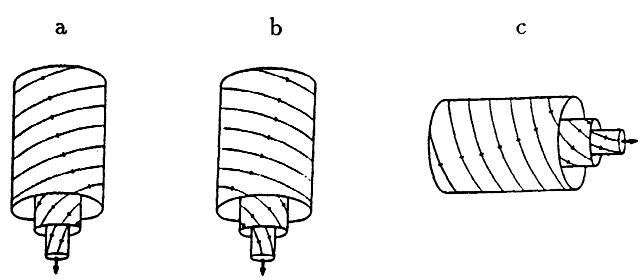

Figure 3. Conceptual diagram of the magnetic field configuration of the magnetic flux ropes that can be used to interpret the ISEE observations shown in Figure 2.

These observations support the suggestion that the HCS acts as a conduit for outflow from large-scale CMEs [*Crooker et al.,* 1993]. The HCS channels the CME ejecta because the HCS is actually a boundary layer between long-lived open field regions with opposite polarity, and the high electric conductivity of the transient CME ejecta within the layer and the ambient solar wind prevents rapid interpenetration each other. Thus the magnetic field within the ejecta cannot intermix with the ambient spiral IMF. It is important to note that the HCS calculated by using the observed photospheric magnetic field and the PFSS model matches only the unperturbed location of a HCS with variable thickness.

4. Specific Evidence for the Existence of the HCS Near Sunspot Maximum

The existence of the HCS in the corona and interplanetary space near the maximum phase of solar cycle 21 has been investigated by using photospheric magnetic field observations from the WSO and near-ecliptic IMF observations by Pioneer Venus Orbiter (PVO), ISEE 3, Pioneer 11, and Voyagers 1 and 2. The photospheric data were used together with a PFSS model to calculate the location of the HCS at the source surface of 2.5 R_s [*Hoeksema et al.,* 1983]. The calculated large-scale magnetic polarity structure was found to be in almost continuous evolution but agrees with the daily IMF polarity observed by ISEE 3 reasonably well during the late rising, maximum, and early declining phases of cycle 21. The current sheet appeared to be highly inclined to the equator during the late rising and early declining phases and even more complex, reaching close to the poles, near maximum. Multipoint observations by ISEE 3 and Pioneer 11 [*Smith et al.,* 1986] and by PVO and Voyagers 1 and 2 [*Behannon et al.,* 1989] show that after application of an appropriate smoothing technique, such as the dominant polarity editing procedure or the computation of a 5-day running average of 12-hour- or 24-hour-averaged IMF polarities, a simple two-sector or occasionally four-sector structure exists near maximum, consistent with the PFSS model predictions.

These studies show the possible existence of the HCS near the maximum phase of solar cycle 21 by statistically comparing the calculated IMF sector pattern with the observed one. It should be noted that this kind of comparison or demonstration provides relatively weak evidence for the existence of the HCS because during this period (1) the HCS is supposed to be highly inclined and most spacecraft sample only the narrow region around the solar equator [*Hoeksema et al.,* 1983] and (2) the model assumptions may be violated owing to the frequency of magnetic flux emergence. To further validate the accuracy of the PFSS model for predicting the magnetic structure of the corona (and therefore the location of the HCS) near the sunspot maximum, we compare the prediction of the coronal magnetic field not only with the observed in-ecliptic IMF polarity, but also with the white light image of the February 16, 1980, solar eclipse that provides some three-dimensional information about the coronal magnetic field.

The high frequency of CMEs and the short duration of coronal holes raise the question of whether a stable spiral IMF exists at all near sunspot maximum. We analyze the histograms of observed hourly IMF azimuthal and latitudinal angles for each rotation from 1978 to 1982 (CR 1671–1724), using the ISEE 3 data. Figure 4 shows that the field direction peaks near both the inward (315°) and outward (135°) spiral directions for all rotations but CR 1695 and CR 1713. The histograms of the IMF latitude (not shown here) also show a most probable value of 0°, confirming the existence of the spiral IMF during the period.

To test the existence of the HCS in CR 1695 and CR 1713, we survey the magnetic field and plasma properties in the two rotations (Figure 5). Also shown are the observed physical properties for CR 1691 when the February 16, 1980, solar eclipse occurred. From top to bottom the panels show the histogram of IMF azimuthal angles, the histogram of latitudinal angles, the calculated location of the HCS and the observed daily IMF polarity, and the observed hourly azimuthal angle and counterstreaming halo electron events. Figure 5 indicates that even the disappearance of the double-peak pattern in the azimuthal angle histogram in CRs

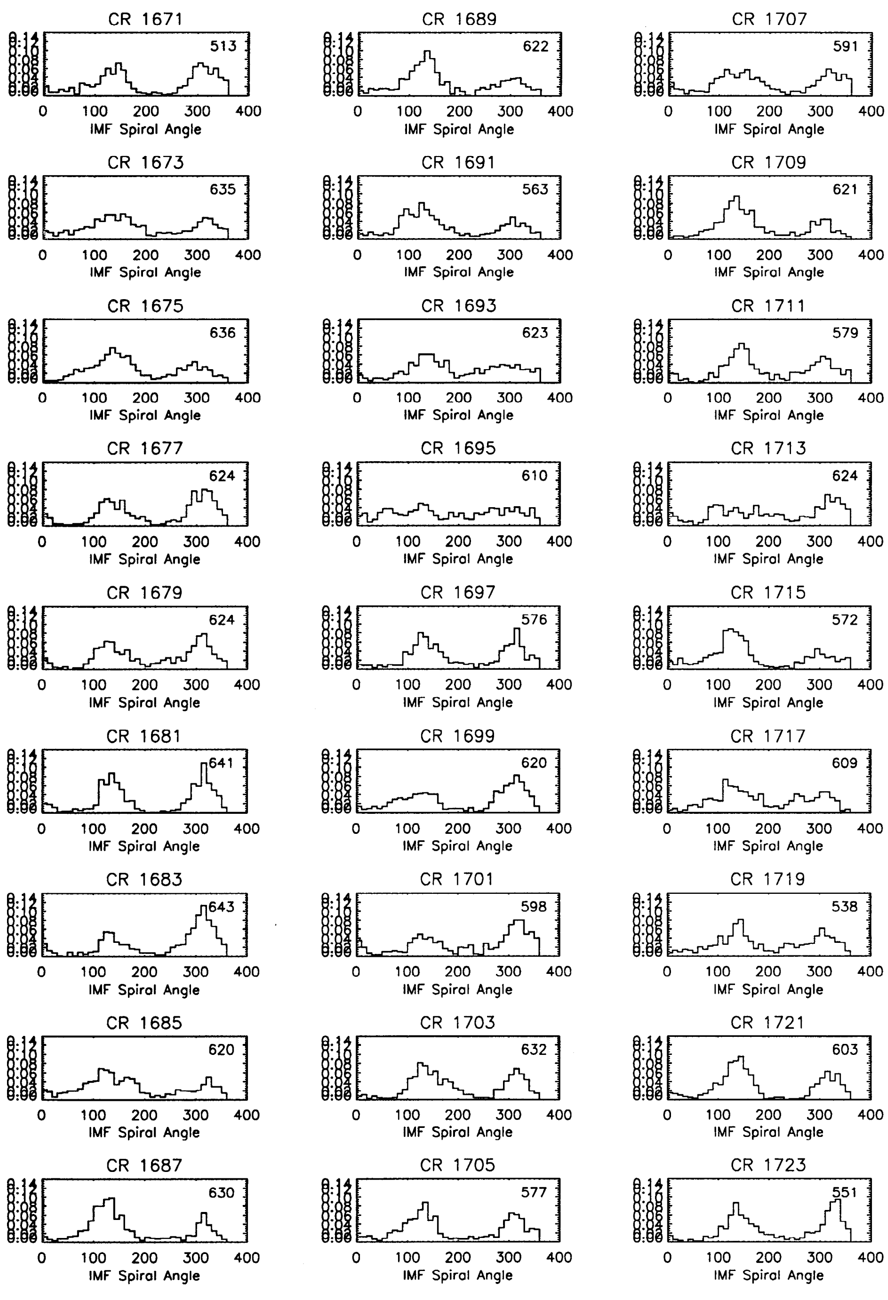

Figure 4. Histogram of hourly averaged IMF azimuthal angles for Carrington rotations from 1978 to 1982. The number within each panel is the number of samples.

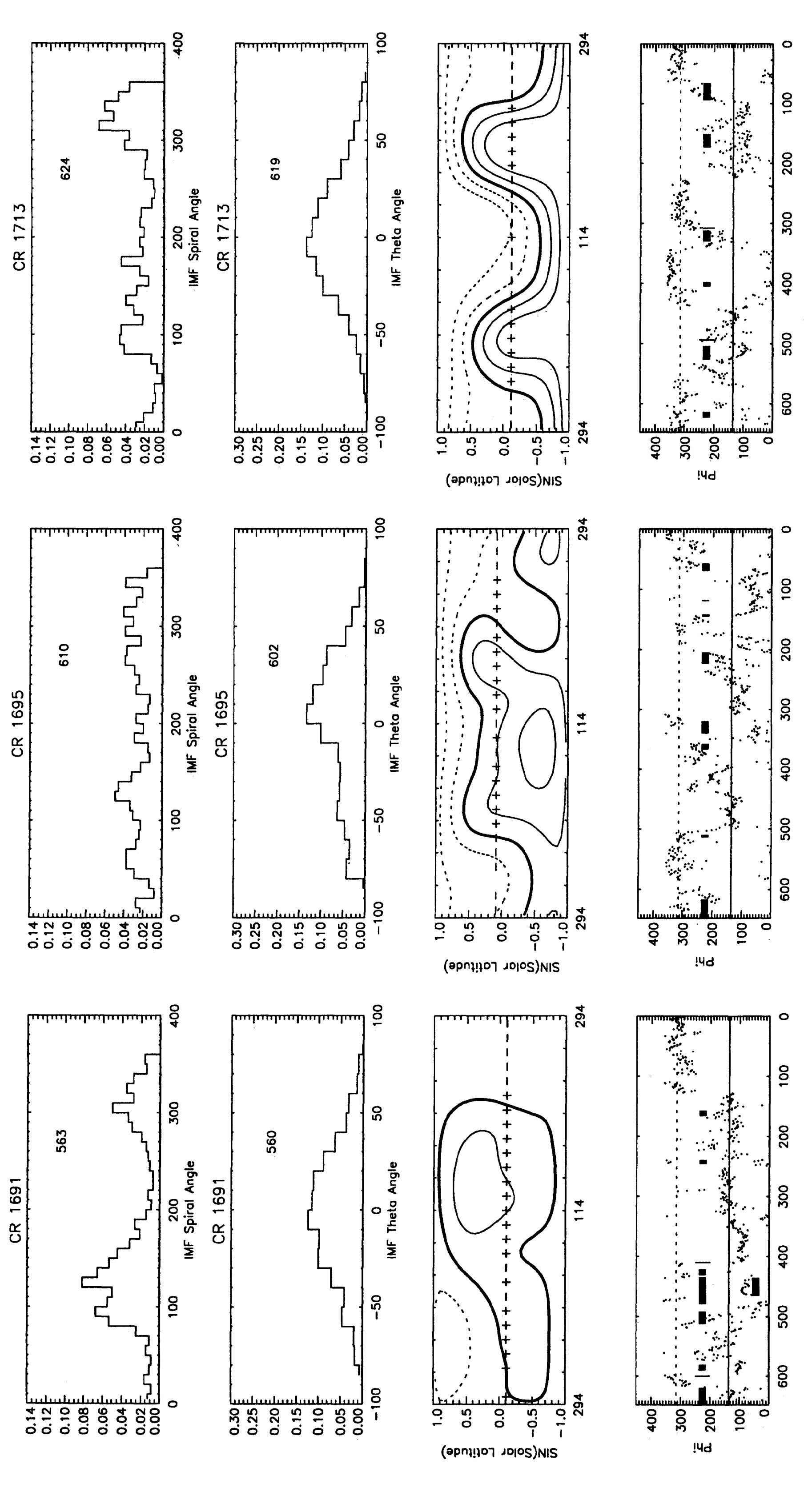

Figure 5. Detailed analysis for Carrington rotations 1691, 1695, and 1713. Panels in top two rows are histograms of the IMF azimuthal and latitudinal angles. Panels in third row show the calculated HCS and observed daily IMF polarity. The fourth row displays observed hourly IMF azimuthal angles and counterstraming halo electron events.

1695 and 1713 does not necessarily imply the disappearance of the HCS because (1) the observed daily IMF polarities show a sector pattern that agrees with the pattern of the calculated HCS and (2) the calculated HCS varies slowly and smoothly from 1694 to 1696 and from 1712 to 1714 (not shown here). The disappearance of the bimodal pattern in CR 1695 and CR 1713 may be understood if the spacecraft frequently crossed magnetic ropes embedded within the heliospheric current layer that separates adjacent IMF polarity sectors. The fourth panel from the top in fact shows that more than seven ICMEs occurred in each of these rotations.

The left column of Figure 5 shows physical properties for CR 1691 (January 24 to February 20, 1980). The histograms of IMF azimuthal and latitudinal angles manifest the well-defined spiral field signature, and the predicted IMF polarities agree very well with observations. Both support the existence of a real HCS structure in the time interval very close to the sunspot maximum (December 1979). To determine the three-dimensional form of the coronal field, we calculate the magnetic field lines in the corona as they would have appeared on February 16, 1980. Unfortunately, the shape of the HCS was too complex in the period to make direct comparison of the calculated HCS with coronal streamers in the eclipse image possible [*Saito et al.,* 1993]. However, it is possible to compare bright regions in the solar eclipse image with the magnetically closed regions in the model. We emphasize that what one sees in optical images is not the magnetic field itself, but electron density structures that roughly outline the shape of field lines; only certain field lines are bright, depending on complex wave and heating processes, with fluctuating, "hidden" boundary conditions determining the localized mass and energy input in the photosphere [*Stenflo,* 1994]. In addition, the white light brightness in the eclipse image shows the integrated electron density along the line of sight. The top panel of Figure 6 displays the field lines originating on an evenly spaced grid in the photosphere, i.e., a grid with equal steps of 10° in latitude and longitude. Using this grid produces distinguishable helmets, but the probability of reproducing all the small streamers in detail is small (especially at maximum), though most of the large helmets are supposed to be accompanied by streamers. The bottom panel displays the observed structure of the white light corona on February 16, 1980, adapted from Figure 1 of *Badalyan et al* [1993]. Coronal loops and arches in the inner corona are indicated by bold lines. *P* indicates prominences, and *D* dark features. Numbers refer to streamers. Subjective visual comparison indicates that most of the observed helmets with streamers 1, 3, 5–9, 11–14, 18, 19, 25, 26, 31–35, and 37 are indeed predicted. This finding supports the validity of the model calculation of the coronal structure at solar maximum in three dimensions and gives additional confidence in the prediction of the location of the HCS.

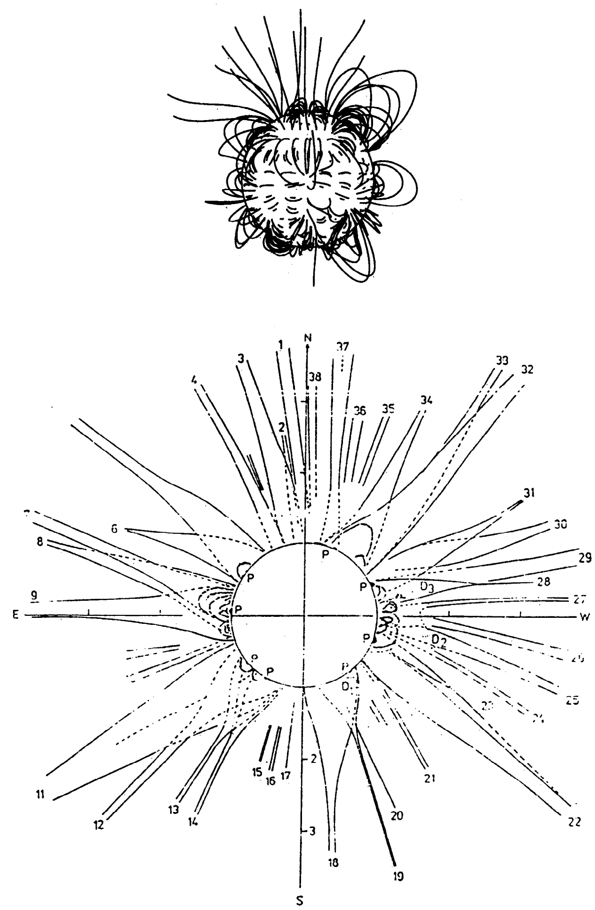

Figure 6. Comparison of the (top) calculated coronal field lines with the (bottom) coronal structure observed in the February 16, 1980, solar eclipse image [from *Badalyan et al.,* 1993]. Most of the calculated closed field regions correspond to the observed helmets with a streamer.

The heliospheric current sheet during sunspot maximum is more complex than a simple inclined current sheet [*Smith et al.,* 1986]. To show the three-dimensional view of the unperturbed heliospheric current sheet near sunspot maximum, Figure 7 depicts the model HCS extending from 2.5 R_s to 5.0 R_s. Each panel indicates the disk center Carrington longitude (cmp) and latitude (lat). The February 16, 1980, eclipse image corresponds to the panel with cmp = 58 and lat = 0. The left and right columns of Figure 7 show the perspective view of an observer located at solar equator and the northern solar pole, respectively. It should be noted that Figure 7 shows only the unperturbed location of the HCS. During the passage of CMEs the current layer may be temporarily and locally distended by CMEs.

5. Summary and Discussion

Virtually no significant permanent changes in the location of the coronal streamer belt or the heliospheric current sheet were observed after blowout CMEs or dis-

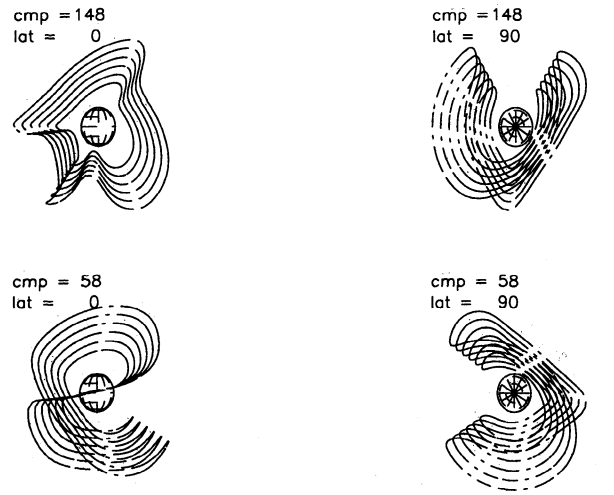

Figure 7. The three-dimensional view of the "average" heliospheric current sheet near sunspot maximum. The values of "cmp" and "lat" denote the Carrington longitude and heliographic latitude of the observer.

ruption CMEs in the late declining phase of solar cycle 21. This finding implies the insensitivity of the photospheric magnetic field to CMEs and the reformation of the blown-out or disrupted preexisting helmet structure in a time shorter than the lifetime of the heliospheric current sheet structure. The reformation time is probably only a couple of days. The HCS, as a global structure, shares the lifetime of large-scale open field regions.

Temporary changes of IMF sector boundaries accompanying counterstreaming halo electron events may be explained as an expansion of sector boundary width and visualized as magnetic ropes propagating between large-scale open field regions with opposite magnetic polarity. These ropes have axes locally parallel to the neutral line or the location of HCS at 1 AU. The HCS can be thought of as an IMF polarity transition layer of variable thickness. Thus the HCS may be useful as a time marker in identifying the interplanetary counterparts of CMEs.

The histograms of observed hourly IMF azimuthal and latitudinal angles for each rotation from CR 1671 to CR 1724 show the maintenance of the spiral characteristics of the interplanetary magnetic field for almost every solar rotation around the maximum phase of solar cycle 21. In addition to the agreement between the calculated and observed IMF sector patterns at maximum, the similarity between the calculated closed field regions and bright structures seen in the February 16, 1980, solar eclipse image further confirms that the three-dimensional structure of the corona is relatively stable and correctly simulated by the model and that the HCS, as a global structure, appears to exist in maximum, even though the HCS may not be a simple sheetlike structure.

The results of sections 2 and 3 show that in other phases of solar cycle, both coronal helmet streamers and well-defined interplanetary sector boundaries reform in a time interval much shorter than the duration of coronal holes [*Burton et al.,* 1994]. The evidence suggests this is true at maximum as well. Since large-scale coronal open field regions (or coronal holes) still exist at maximum and their lifetimes are greater than the reformation time of large-scale closed field regions (or helmet streamers), the stable spiral orientation of the IMF and the stable HCS is expected, even during the time when CMEs occur frequently and many of the coronal helmet streamers along the base of the sheet are disrupted or blown out. The large open field regions that create a stable HCS during other phases of the cycle are replaced by smaller open field regions scattered over a wide range of latitudes during sunspot maximum [*Wang and Sheeley,* 1994]. Because the open field regions in the maximum phase occupy a relatively small fraction of the solar surface, their field lines must expand on the average more rapidly in the corona. Consequently, the wind speed produced by using the method of *Wang and Sheeley* [1994] should be dominated by wind speeds lower than 450 km s^{-1}. This prediction is consistent with observations and may provide another confirmation of the accuracy of the calculated open field regions and thus the existence of the HCS in the maximum phase. Ulysses observations at the next sunspot maximum may finally help to determine whether the HCS exists throughout the solar cycle.

Acknowledgments. We thank J. T. Gosling for providing the list of counterstreaming halo electron events and shocks and A. J. Hundhausen and J. T. Burkepile for the catalogue of SMM coronal mass ejections used in this study. This work was supported by the National Aeronautics and Space Administration under grant NGR5-020-559, by the Atmospheric Sciences Section of the National Science Foundation under grant ATM90-22249, and by the Office of Naval Research under grant N00014-89-J-1024.

The Editor thanks two referees for their assistance in evaluating this paper.

References

Badalyan, O. G., M. A. Livshits, and J. Sykora, Polarization of the white-light corona and its large-scale structure in the period of solar cycle maximum, *Sol. Phys.,145*, 279, 1993.

Behannon, K. W., L. F. Burlaga, T. J. Hoeksema, and L. W. Klien, Spatial variation and evolution of heliospheric sector structure, *J. Geophys. Res., 94*, 1245–1260, 1989.

Burkepile, J. T., and O. C. St. Cyr, *A Revised and Expanded Catalogue of Mass Ejections Observed by the Solar Maximum Mission Coronagraph*, High Altitude Obs., Natl. Cent. for Atmos. Res., Boulder, Colo., 1993.

Burlaga, L. F., A. J. Hundhausen, and X. P. Zhao, The coronal and interplanetary current sheet in early 1976, *J. Geophys. Res., 86*, 8893, 1981.

Burton, M. E., N. U. Crooker, G. L. Siscoe, and E. J. Smith, A test of source-surface model predictions of heliospheric current sheet inclination, *J. Geophys. Res., 99*, 1–9, 1994.

Crooker, N. U., G. L. Siscoe, S. Shodhan, D. F. Webb, J. T. Gosling, and E. J. Smith, Multiple heliospheric current sheets and coronal streamer belt dynamics, *J. Geophys. Res., 98*, 9371–9381, 1993.

Gosling, J. T., Coronal mass ejections and magnetic flux ropes in interplanetary space, in *Physics of Magnetic Flux Ropes, Geophys. Monogr. Ser.,* Vol. 58, edited by C. T. Russell, E. R. Priest, and L. C. Lee, pp.343–364, AGU, Washington, D. C., 1990.

Hiei, E., A. J. Hundhausen, and D. G. Sime, Reformation of a coronal helmet streamer by magnetic reconnection after a coronal mass ejection, *Geophys Res. Lett., 20*, 2785–2788, 1993.

Hoeksema, J. T., Large-scale structure of the heliospheric magnetic field: 1976–1991, *Adv. Space Res., 9*, 15, 1991.

Hoeksema, J. T., and X. P. Zhao, Prediction of coronal and interplanetary magnetic fields using the current sheet–source surface model, *J. Geomagn. Geoelectr.,* in press, 1996.

Hoeksema, J. T., J. M. Wilcox, and P. H. Scherrer, The structure of the heliospheric current sheet in the early portion of sunspot cycle 21, *J. Geophys. Res., 87*, 10,331–10,338, 1982.

Hoeksema, J. T., J. M. Wilcox, and P. H. Scherrer, The structure of the heliospheric current sheet: 1978–1982, *J. Geophys. Res., 88*, 9910–9918, 1983.

Howard, R. A., N. R. Sheeley Jr., M. J. Koomen, and D. J. Michels, Coronal mass ejections: 1979–1981, *J. Geophys. Res., 90*, 8173–8192, 1985.

Hundhausen, A. J., Coronal observations: Getting to the bottom of the heliospheric current sheet (abstract), *Eos Trans AGU, 73*(43), Fall Meet. Suppl., 431, 1992.

Hundhausen, A. J., Sizes and locations of coronal mass ejections: SMM observations from 1980 and 1984–1989, *J. Geophys. Res., 98*, 13,177–13,200, 1993.

Ness, N. F., and J. M. Wilcox, Solar origin of the interplanetary magnetic field, *Phys. Res. Lett., 13*, 13,461, 1964.

Saito, T., S.-I. Akasofu, Y. Kozuka, T. Takahashi, and S. Numazawa, The solar coronal sheet during the period of sunspot maximum, *J. Geophys. Res., 98*, 5639, 1993.

Schulz, M., Interplanetary sector structure and the heliomagnetic equator, *Astrophys. Space Sci., 24*, 371, 1973.

Smith, E. J., B. Tsurutani, and R. L. Rosenberg, Observations of the interplanetary sectors structure up to heliographic latitudes of 16°: Pioneer 11, *J. Geophys. Res., 83*, 717, 1978.

Smith, E. J., J. A. Slavin, and B. T. Thomas, The heliospheric current sheet: 3–Dimensional structure and solar cycle changes, in *The Sun and the Heliosphere in Three Dimensions*, edited by R. G. Marsden, pp. 267–274, D. Reidel, Dordrecht, 1986.

Stenflo, J., *Solar Magnetic Field*, 385 pp., D. Reidel, Dordrecht, 1994.

Suess, S., The relationship between coronal and interplanetary magnetic fields, *Adv. Space Res., 13*(9), 31, 1993.

Wang, Y.-M., and N. R. Sheeley Jr., On potential field models of the solar corona, *Astrophys. J., 392*, 310, 1992.

Wang, Y.-M., and N. R. Sheeley Jr., Global evolution of interplanetary sector structure, coronal holes, and solar wind streams during 1976–1993: Stackplot displays based on solar magnetic observations, *J. Geophys. Res., 99*, 6597–6608, 1994.

Wilcox, J. M., and A. J. Hundhausen, Comparison of heliospheric current sheet structure obtained from potential magnetic field computations and from observed polarization coronal brightness, *J. Geophys. Res., 88*, 8095–8096, 1983.

Wilcox, J. M., and N. F. Ness, Quasi-stationary corotating structure in the interplanetary medium, *J. Geophys. Res., 70*, 5793, 1965.

Wilcox, J. M., P. H. Scherrer, and J. T. Hoeksema, The origin of the warped heliospheric current sheet, *Science, 209*, 603, 1980.

Zhao, X. P., and J. T. Hoeksema, Unique determination of model coronal magnetic fields using photospheric observations, *Sol. Phys., 143*, 41–48, 1993.

Zhao, X. P., and J. T. Hoeksema, Prediction of interplanetary magnetic field strength, *J. Geophys. Res., 100*, 19–33, 1995.

X. P. Zhao and J. T. Hoeksema, H.E.P.L B204, Center for Space Science and Astrophysics, Stanford University, Stanford, CA 94305-4085. (e-mail: xpzhao@solar.stanford.edu; jthoeksema@solar.stanford.edu)

(Received February 9, 1995; revised November 20, 1995; accepted November 20, 1995.)